(2)

IMENTATION PAGE

Form Approved
OMB No. 0704-0188

AD-A264 749

2. REPORT DATE	3. REPORT TYPE AND DATES COVERED
19 February 1993	Final - 1 Jan. 88 to 31 Dec. 92

4. TITLE AND SUBTITLE

X-Ray Absorption Spectroscopy of Electrochemically Generated Species

5. FUNDING NUMBERS

AFOSR 88-0089

6. AUTHOR(S)

William R. Heineman
Richard C. Elder

7. PERFORMING ORGANIZATION NAME(S) AND ADDRESS(ES)

University of Cincinnati
Department of Chemistry
Cincinnati, Ohio 45221-0172

AFOSR

8. PERFORMING ORGANIZATION REPORT NUMBER

9. SPONSORING/MONITORING AGENCY NAME(S) AND ADDRESS(ES)

AFOSR
110 Duncan Avenue, Suite B115
Bolling AFB
D.C. 20332-0001

NC

10. SPONSORING/MONITORING AGENCY REPORT NUMBER

11. SUPPLEMENTARY NOTES

12a. DISTRIBUTION/AVAILABILITY STATEMENT

Approved for public release;
distribution unlimited.

93-10748

93 5 13 045

13. ABSTRACT *(Maximum 200 words)*

X-ray absorption fine structure (EXAFS) spectroscopy has been combined with electrochemistry to enable the measurement of coordination numbers, donor atom types and bond lengths of metal ions in multiple oxidation states which are generated electrochemically. We have demonstrated the applicability of this technique to study the redox coordination chemistry of metal ions in aqueous and nonaqueous solvents, ionically conducting polymer films, electroactive films on conducting metals and electrically conducting polymers. Our objectives were to conduct research in the following areas: (1) electrostatic cross-linking of ionic polymer films and their effects on the structures of charged coordination compounds immobilized in the film, (2) cation charge transport and its effects on the structures of electroactive films such as Prussian blue deposited on electrodes, (3)metal ions incorporated in electrically conducting polymers, (4) development of a flow cell which enables EXAFS spectroelectrochemistry to be performed in a controlled atmosphere environment, (5) structure determination for metals and intermetallic compounds in mercury solvent, and (6) evaluation of spectroelectrochemical nernstian plots.

14. SUBJECT TERMS	15. NUMBER OF PAGES
X-ray absroption, electrochemistry	16. PRICE CODE

17. SECURITY CLASSIFICATION OF REPORT	18. SECURITY CLASSIFICATION OF THIS PAGE	19. SECURITY CLASSIFICATION OF ABSTRACT	20. LIMITATION OF ABSTRACT
unclassified	unclassified	unclassified	

COMPLETED PROJECT SUMMARY

TITLE: X-Ray Absorption Spectroscopy of Electrochemically Generated Species

PRINCIPAL INVESTIGATORS: Professor William R. Heineman
Professor Richard C. Elder
Department of Chemistry
University of Cincinnati
Cincinnati, OH 45221-0172

INCLUSIVE DATES: 1 January 1988 - 31 December 1992

CONTRACT/GRANT NUMBER: AFOSR 88-0089

COSTS AND FY SOURCE: $136,307, FY 88; $135,051, FY 89
$126,535, FY 90, FY 91, FY 92

SENIOR RESEARCH PERSONNEL:

Dr. Lee Sharpe
Dr. Eric Kristensen
Dr. Yingping Deng
Dr. John D'Amore

JUNIOR RESEARCH PERSONNEL:

David Igo
Rob Tieman
Robert Rigney

PUBLICATIONS:

The Electrochemistry of Hemin in Dimethylsulfoxide. R.S. Tieman, L.A. Coury, Jr., J.R. Kirchhoff, W.R. Heineman, J. Electroanal. Chem. **281**, 133-145 (1990).

EXAFS Spectroelectrochemistry. L.R. Sharpe, R.C. Elder, W.R. Heineman, Chem. Rev. **90**, 705-722 (1990).

EXAFS Solid-State Spectroelectrochemistry: Effects of Supporting Electrolyte on the Structure of $Cu(bcp\text{-}s)_2^{3-}$. D.H. Igo, R.C. Elder, W.R. Heineman. J. Electroanal. Chem., **314**, 45-57 (1991).

Non-Ideal Behavior of Nernstian Plots from Spectroelectrochemistry Experiments. E.W. Kristensen, D.H. Igo, R.C. Elder, W.R. Heineman. J. Electroanal. Chem., **309**, 61-72 (1991).

Development of a Bulk-Electrolysis Flow-Cell System for UV-Visible and X-Ray Absorption Spectroelectrochemical Analysis. D.H. Igo, R.C. Elder, W.R. Heineman, and H.D. Dewald, Anal. Chem., **63**, 2535-2539 (1991).

ABSTRACT OF OBJECTIVES AND ACCOMPLISHMENTS:

X-ray absorption fine structure (EXAFS) spectroscopy has been combined with electrochemistry to enable the measurement of coordination numbers, donor atom types and bond lengths of metal ions in multiple oxidation states which are generated electrochemically. We have demonstrated the applicability of this technique to study the redox coordination chemistry of metal ions in aqueous and nonaqueous solvents, ionically conducting polymer films, electroactive films on conducting metals and electrically conducting polymers. Our objectives were to conduct research in the following areas: (1) electrostatic cross-linking of ionic polymer films and their effects on the structures of charged coordination compounds immobilized in the film, (2) cation charge transport and its effects on the structures of electroactive films such as Prussian blue deposited on electrodes, (3)metal ions incorporated in electrically conducting polymers, (4) development of a flow cell which enables EXAFS spectroelectrochemistry to be performed in a controlled atmosphere environment, (5) structure determination for metals and intermetallic compounds in mercury solvent, and (6) evaluation of spectroelectrochemical nernstian plots.

1. Coordination Compounds in Ionically Conducting Polymer Films

A major objective has been to demonstrate that EXAFS spectroelectrochemistry is applicable to the study of metal complexes immobilized in polymer films on electrode surfaces. We have demonstrated this with two ionic polymers: Nafion and poly(dimethyldiallylammonium chloride), PDMDAAC.

We have examined $[Cu^{I}(dmp)_2]^{+}$ (dmp = 2,9-dimethyl-1,10-phenanthroline) incorporated into a Nafion polymer. The Cu-N bond length decreased from 2.06Å to 2.02Å and the coordination number increased from 4 to 5 when the Cu^{II} species was generated by application of a positive potential to the gold film electrode. This increase in coordination number is attributed to a change of coordination geometry from a tetrahedral (4-coordinate) to a trigonal bipyramidal (5-coordinate) arrangement.

Our results for $[Cu^{I}(bcp\text{-}s)_2]^{-3}/[Cu^{II}(bcp\text{-}s)_2]^{-2}$ where bcp-s = 2,9-dimethyl-4,7-diphenyl-1,10-phenanthroline disulfonic acid disodium salt in p(DMDAAC) are extremely interesting with respect to the effect of the polymer environment on the structures of the two redox forms of the copper complex: namely, in aqueous solution $[Cu^{I}(bcp\text{-}s)_2]^{-3}$ exists as a tetrahedral complex which converts, with the addition of a fifth ligand, to a trigonal bipyramid when oxidation to $[Cu^{II}(bcp\text{-}s)_2(H_2O)]^{-2}$ occurs; whereas, in the polymeric

film, p(DMDAAC), the tetrahedral structure is observed for both oxidation states. The polymer environment apparently prevents the structural change associated with electron transfer that occurs in aqueous environment.

2. Metal Ions in Electroactive Films on Conducting Metals: Prussian Blue

Electrodes modified by hexacyanometalate films formed from various metals, such as Prussian Blue (PB), have been shown to have interesting electrochemical and spectral properties. Due to the complex environments about the iron centers, determination of the structures of these electrochemically generated materials is very difficult. High quality X-ray fluorescence spectra have been collected on each of three electrochemically generated oxidation states. The Fourier transforms of the EXAFS indicate Fe-Fe interactions. A decrease of the iron backscattering interaction is attributed to distortions of the cage structure of PB upon its reduction. Such distortion likely occurs when the cage has to incorporate hydrated cations to counterbalance the charge that accumulates upon decreasing the overall charge on iron.

3. Electrically Conducting Polymers: Copper in Poly(3-Methylthiophene)

Electrically conducting polymers with extended π-electron systems have been a subject of interest in recent years. Our EXAFS studies have involved investigation of the chemical and structural form of the copper ions in the insoluble polymer matrix of poly(3-methylthiophene). This study provides insight concerning the role of the copper in the conduction process. In the non-conductive system, the copper contained within the p(3-methylthiophene) matrix complexes water. This complexation causes a distortion in the orientation of the thiophene array, thereby disrupting the π-electron conductivity present in the absence of water.

4. EXAFS Spectroelectrochemical Flow-Cell

We have shown that electrolysis offers a practical alternative to chemical generation of chosen oxidation states. For EXAFS measurements potential control may be necessary to maintain the oxidation state of the metal being observed, due to the highly reducing environment generated by secondary electrons produced by the intense synchrotron radiation. We have built and evaluated a cell which combines both electrochemical potential control and a flowing analyte stream. A packed carbon-bed bulk electrolysis cell generates the desired metal oxidation state. Complete oxidation and reduction of a 10 mM solution of $K_3Fe(CN)_6$ can be achieved with only one electrolysis pass.

5. Structure of Metals in Amalgams.

The characteristics of amalgams have been extensively analyzed with a variety of techniques. Based upon electrochemical measurements, it has been proposed that several $metal_1$-$metal_2$ complexes will form in amalgams. The solubility of these intermetallic compounds in mercury is frequently low and the solid phase separates. Interestingly, in many cases, structures of these complexes are not known. The feasibility of EXAFS spectroelectrochemistry on metals dissolved in mercury has been evaluated with a preliminary experiment on zinc. These preliminary experiments have shown that sufficient zinc atoms can be electrochemically preconcentrated in an electrochemically generated mercury film to collect X-ray absorption data with relatively high signal to noise. Based on observations of the XANES region of the X-ray absorption spectrum we have revealed a distinct difference in the features of the amalgam spectrum, collected at the zinc edge, as compared to both zinc metal and hexaaquozinc(II) diacetate. The amplitude and phase features of the filtered EXAFS signal are characteristic of mercury coordinated to zinc at 3.0 Å.

6. Non-Ideal Behavior of Spectroelectrochemical Nernstian Plots

Analysis of Nernstian plots has been shown to be a powerful technique for determining the formal redox potentials and electron stoichiometries of various electroactive species. However, in certain situations nonlinear Nernstian plots have been observed. Consequently, analysis by conventional methodologies results in erroneous estimation of these redox parameters. We have explored the chemical basis for the observed deviation and presented a model which predicts this behavior. The validity of the chemically independent redox model was demonstrated using thin-layer spectroelectrochemistry with two well characterized spectroelectrochemical systems: ferricyanide and σ-tolidine.

X-RAY ABSORPTION SPECTROSCOPY OF ELECTROCHEMICALLY GENERATED SPECIES

William R. Heineman and Richard C. Elder
Department of Chemistry
University of Cincinnati
Cincinnati, OH 45221-0172

18 February 1993

Final Report for Period 1 January 1988 - 31 December 1992

Prepared for:

Air Force Office of Scientific Research
110 Duncan Avenue
Suite B115
Bolling Air Force Base, DC 20332-0001

John S. Wilkes
Program Manager
Directorate of Chemical and Atmospheric Sciences

Final Technical Report

During the past four years our research, with the support of AFOSR 88-0089, has been focused on the use of EXAFS spectroelectrochemistry to investigate and characterize the coordination environment of transition metal complexes which undergo electron transfer reactions. We have studied these materials in bulk solution or incorporated in polymer films on electrode surfaces. We have also investigated complexes contained within an ionically conducting polymer electrolyte matrix. In order to obtain good EXAFS spectra of these systems, we have developed several new cell designs. In all cases the EXAFS spectroelectrochemical experiments have been preceded by extensive characterization of the coordination compounds and polymer systems by cyclic voltammetry, coulometry, and uv-visible spectroelectrochemistry. These experiments are all done at the University of Cincinnati, whereas EXAFS is measured at one of the national laboratories.

1. Coordination Compounds in Ionically Conducting Polymer Films

A major objective of our recent work has been to demonstrate that EXAFS spectroelectrochemistry is applicable to the study of metal complexes immobilized in polymer films on electrode surfaces. We have demonstrated this with two ionic polymers: Nafion and poly(dimethyldiallylammonium chloride).

a. $Cu(dmp)_2^{+1,+2}$ in Solution and in Nafion.

Perhaps the most extensively studied polymer for modified electrodes is the water insoluble cation exchange membrane Nafion. The practical importance of Nafion lies partly in its use as a protective coating. As an overlying membrane, Nafion provides both size exclusion and a charge selective barrier. The size selectivity of the polymer matrix is determined by the hydrocarbon chain length. The ability to change the molecular weight of the Nafion repeat unit allows partitioning into the film based on size. The sulfonate group enables the polymer to selectively allow both neutral and positively charged materials of the appropriate size to permeate through or be incorporated into the matrix (1). Electrodes coated with Nafion can then be used to competitively select and detect charged and neutral electroactive materials. A good example is its use as a coating for ultra-microelectrodes for the in vivo detection of neurotransmitters (2).

We have examined $[Cu^{I}(dmp)_2]^{+}$ (dmp = 2,9-dimethyl-1,10-phenanthroline) incorporated into a Nafion polymer (3). The spectroelectrochemical cell had a gold film electrode vapor deposited on a Mylar sheet. Co-dissolved colloidal

graphite and Nafion in ethanol/ethylacetate was sprayed onto the gold to give a ~0.1 mm-thick polymer film. The nafion-coated electrode was then contacted with electrolyte containing $[Cu^{I}(dmp)_2]^{+}$, which partitioned from aqueous solution into the negatively charged Nafion. High quality EXAFS spectra were obtained for $[Cu^{I}(dmp)_2]^{+}$ in the Nafion film by measuring the fluorescence signal passing through the electrode.

We reported that the Cu-N bond length decreased from 2.06Å to 2.02Å and the coordination number increased from 4 to 5 when the Cu^{II} species was generated by application of a positive potential to the gold film electrode. This increase in coordination number is attributed to a change of coordination geometry from a tetrahedral (4-coordinate) to a trigonal bipyramidal (5-coordinate) arrangement. The added ligand is most likely coordinated through oxygen, either from a sulfonate group in Nafion or a water molecule present in the polymer matrix. This experiment clearly showed that EXAFS has sufficient sensitivity for the study of metal ions in thin polymer films on electrode surfaces.

b. $Cu(bcp\text{-}s)_2^{-3,-2}$ in Solution and in p(DMDAAC).

Electrochemical cells in which the traditional supporting electrolyte consists of ionically-conducting, semi-rigid polymer films for solid-state voltammetry have been reported (4-6). Such electrochemical cells enable gas phase detection of electroactive species (7,8). The water soluble polymer, poly(dimethyldiallylammonium chloride) or p(DMDAAC) is an example of this type of polymer.

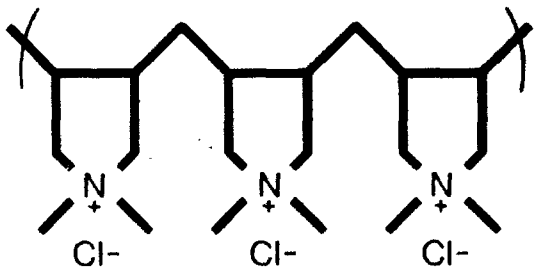

The uses and characteristics of p(DMDAAC) as an ionically conducting polymer film have been investigated extensively in our laboratories (6,8-11).

In our EXAFS spectroelectrochemistry experiment, p(DMDAAC) not only physically contains the metal complex in the X-ray beam but also acts as the electrolyte during electrochemical conversion from one oxidation state to another (11). The electrochemical cell (Fig. 1) consists of a gold minigrid optically transparent thin-layer working electrode, two platinum foil auxiliary electrodes, and an oxidized silver wire reference electrode. The electrochemical cell components are attached to a Mylar window. A solution of the complex and p(DMDAAC) is cast onto the electrochemical cell and allowed

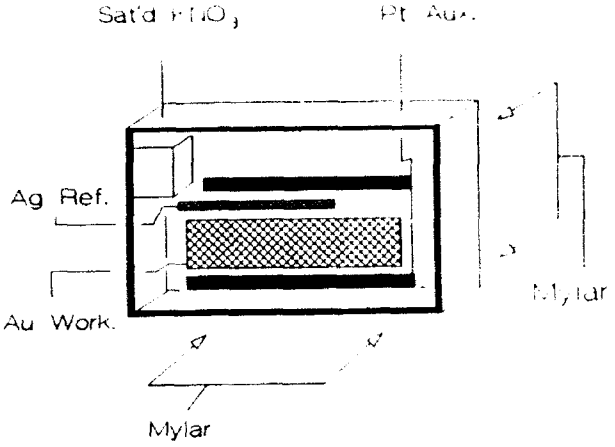

to dry. In order to provide the required ionic-conductivity, the completed electro-chemical cell is encased in a chamber with a saturated aqueous potassium nitrate solution (~2 mL) that maintains a constant relative humidity of 92.5% (12). This cell can then be placed perpendicular to the light path of our diode array spectrometer for uv-visible spectroelectrochemistry or positioned 45° with respect to the X-ray beam inside our Lytle X-ray fluorescence detector for obtaining X-ray absorption spectra.

The constant humidity electrochemical cell provides some unique advantages: (a) the experiment is done in the absence of supporting electrolyte and (b) the metal complex is concentrated within a thin polymer film (~0.05 mm). With no supporting electrolyte, the behavior of the complex can be analyzed in the presence of only the polymer film. This also minimizes attenuation of the X-ray beam by electrolyte absorption. Concentration of the complex at the electrode surface increases the amount of complex probed by the X-ray beam, increasing the signal to noise ratio. With this electrochemical cell design we have shown that within the polymer film complete electrolysis of a complex occurs. This was demonstrated via double potential step chronoamperometry in conjunction with visible spectroscopy experiments (11). In addition, we have shown that high quality X-ray fluorescence spectra of a copper complex incorporated into a p(DMDAAC) film can be obtained.

In these experiments, the electroactive molecule was $[Cu^{I}(bcp\text{-}s)_2]^{-3}$, where bcp-s = 2,9-dimethyl-4,7-diphenyl-1,10-phenanthroline disulfonic acid disodium salt. The complex possesses a negative charge, thus allowing it to electrostatically interact with the positive charge of p(DMDAAC). The electrochemistry of the complex was evaluated in the semi-rigid polymer film and was found to exhibit an increased degree of reversibility as compared to that in solution.

The ability to access each oxidation state of the complex allows analysis of the structural characteristics of both the Cu^{I} and Cu^{II} oxidation states while in p(DMDAAC). The structures were determined from analysis of our EXAFS spectroelectrochemistry experiment (11), and compared to the results for

solution. Results of these experiments are presented in Table 1, employing $Cu^{I}(dmp)_2BF_4$, where dmp = 2,9-dimethyl-1,10-phenanthroline, as a model compound. Since, dmp and bcp-s have identical phenanthroline backbones, $[Cu^{I}(dmp)_2]BF_4$ should be an ideal model for Cu-N interaction in $Cu(bcp\text{-}s)_2$. When comparing results obtained with the $Cu(bcp\text{-}s)_2$ with those of $Cu(dmp)_2$ solution (3), the Cu-N bond distance remains approximately constant while the $Cu(dmp)_2$ showed an decrease of ~0.04 Å. As with $Cu(dmp)_2$, the number of atoms coordinated to copper increases by 1 or 25% when Cu^{I} complex is oxidized. We believe the absolute values of the coordination number given in Table 1 are incorrect. The disorder parameter, σ, has not been refined and is so highly correlated with the coordination number as to render the absolute value for coordination number meaningless. What is meaningful is the increase in coordination number which results from oxidation. We believe that this represents an increase from four to five coordinate in solution. Most interestingly, no such increase is seen in coordination number as the complex in the polymer film is oxidized to Cu(II).

Table 1 - $Cu(bcp\text{-}s)_2$ in solution and p(DMDAAC) Results

	Cu^{I} State		Cu^{II} State	
System	BL	CN	BL	CN
8.7 mM Solution	2.05	5.90	2.04	7.35
Complex/p(DMDAAC)	2.06	5.12	2.06	5.05

Our results for $[Cu^{I}(bcp\text{-}2)_2]^{-3}/[Cu^{II}(bcp\text{-}s)_2]^{-2}$ in p(DMDAAC) are extremely interesting with respect to the effect of the polymer environment on the structures of the two redox forms of the copper complex: namely, in aqueous solution $[Cu^{I}(bcp\text{-}s)_2]^{-3}$ exists as a tetrahedral complex which converts, with the addition of a fifth ligand, to a trigonal bipyramid when oxidation to $[Cu^{II}(bcp\text{-}s)_2(H_2O)]^{-2}$ occurs; whereas, in the polymeric film, p(DMDAAC), the tetrahedral structure is observed for both oxidation states. The polymer environment apparently prevents the structural change associated with electron transfer that occurs in aqueous environment. Thus, a seemingly innocuous polymer with no coordination sites, whose primary purpose in the electrochemical cell is simply to provide an ionically conducting medium (i.e.

supporting electrolyte) to support charge flow in the electrochemical cell, appears to significantly alter the chemistry of a metal complex.

We attribute this structural anomaly to the role that bulky, negatively charged $[Cu^{I}(bcp\text{-}s)_2]^{-3}/[Cu^{II}(bcp\text{-}s)_2]^{-2}$ plays in electrostatically cross-linking the positively charged DMDAAC polymer. The effect of electrostatic cross-linking is dramatically observable in a swelling experiment. $[Cu^{I}(bcp\text{-}s)_2]^{-3}$ is added to an aqueous solution in which a DMDAAC-coated electrode has been immersed and allowed to swell. Addition of complex to the solution causes the polymer film to shrink by a factor of 10 or more. As the complex diffuses into the film, it ionically interacts with the quaternary ammonium sites, thereby, cross-linking the polymer with an accompanying "squeezing out of water." Apparently, the ionic attraction between positively charged polymer sites and the negatively charged sulfonic acid sites on the ligands is sufficiently strong to hold the complex in a relatively fixed tetrahedral geometry when the copper center is oxidized to Cu^{II}. The size of the bcp-s ligands should also affect the ability of the complex to reorganize. In order for the complex to assume trigonal bipyramidal geometry, the bulky ligands must reorient, placing one nitrogen of a bcp-s ligand in an axial coordination site. For the ligand to move, it must essentially drag along large amounts of polymer as it assumes the new geometry, or substantially increase the separation between anionic and cationic sites.

2. Metal Ions in Electroactive Films on Conducting Metals: Prussian Blue

Electrodes modified by hexacyanometalate films formed from various metals, such as Prussian Blue (PB), have been shown to have interesting electrochemical and spectral properties (13). An electrochemically generated and maintained PB film is potentially useful in electrochromic display devices. Due to the complex environments about the iron centers, determination of the structures of these electrochemically generated materials is very difficult.

Mossbauer, infrared, and optical absorption spectroscopic investigations confirm the fact that the insoluble film is an $iron^{III}$ hexacyanoferrate, $\{Fe^{III}[Fe^{II}(CN)_6]\}^{-}$. X-ray crystallography has been used to characterize the structure of the insoluble crystalline form of the complex (14). Three different crystalline forms, each possessing four unique iron coordination environments, have been found. Upon first inspection, the iron coordination structure of PB appears to be too heterogeneous to practically analyze via EXAFS. yet there is a distinct Fe-Fe separation of 5.08 Å. This distance is

associated with the Fe-C≡N-Fe linkage within the caged structure. The colinearity of the Fe-C≡N-Fe allows direct observation of the separation of the iron centers within the cage of PB at a distance not normally achievable with conventional room temperature EXAFS analysis (15). Although the structure of the PB form of the film is known, little or no information has been obtained concerning the in situ behavior of the electrochemically deposited material and the structure of its oxidized and reduced forms. EXAFS analysis allows evaluation of the distance between the iron atoms of the cage. Electrochemically generated forms of PB include the totally reduced Berlin green (BG) and its totally oxidized state, Everitt's salt (EVS). The electrochemical properties of the compound in its respective states have been described in great detail (16); a representation of the electrochemical reaction is given below:

$$\{Fe^{III}[Fe^{III}(CN)_6]\}^0 \overset{e^-}{\underset{}{\rightleftarrows}} \{Fe^{III}[Fe^{II}(CN)_6]\}^{-1} \overset{e^-}{\underset{}{\rightleftarrows}} \{Fe^{II}[Fe^{II}(CN)_6]\}^{-2}$$

Everitt's salt, (EVS) Prussian blue, (PB) Berlin green, (BG)

Most importantly, the various oxidation states are easily accessed and the products are stable over a long period of time while potential control is maintained.

Our investigations have involved the electrochemical deposition of PB onto a gold film electrode (300 Å thick, vapor-deposited onto Mylar) incorporated into a thin-layer EXAFS spectroelectrochemical cell, described in our recent review (17). The gold film not only provides a suitable electrode material and physical support for PB, but is transparent in both the visible and X-ray spectral regions. High quality X-ray fluorescence spectra have been collected on each of the three generated oxidation states. The Fourier transforms of the EXAFS, (Fig. 2), indicate Fe-Fe interactions. The peak appears at a shorter distance, (~4.5), than the crystal value of 5.08 Å due to the EXAFS phase shift, as expected. A marked decrease in amplitude of the Fe-Fe peak at ~4.5 Å is seen when comparing BG to EVS. The decrease of the iron backscattering interaction is attributed to distortions of the cage structure of PB upon its reduction. Such distortion likely occurs when the cage has to incorporate hydrated cations to counterbalance the charge that accumulates

upon decreasing the overall charge on iron. This is further supported by analysis of the amplitude of the back-transform function of the radial distribution peak associated with the Fe-Fe backscattering interaction (Fig. 3). Upon decreasing the overall charge of the iron within the film, from EVS, to PB and to BG, the peak magnitude decreases.

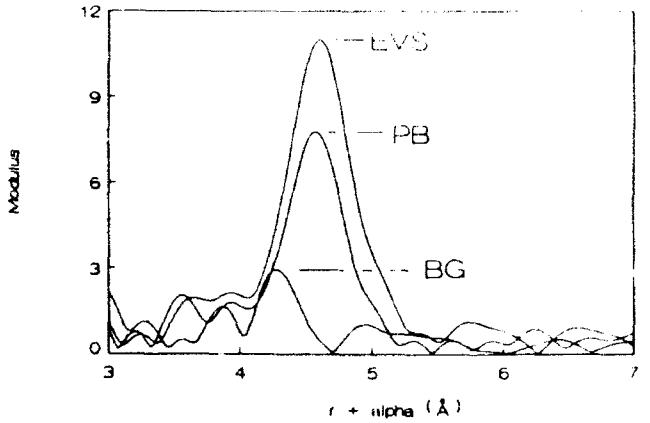

Figure 2

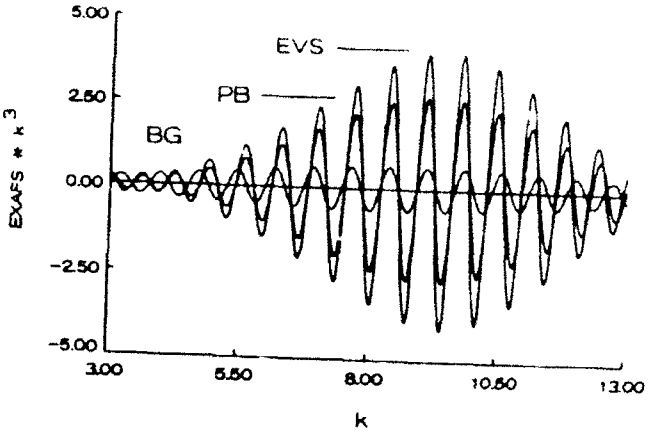

Figure 3

3. Electrically Conducting Polymers: Copper in Poly(3-Methylthiophene)

Electrically conducting polymers with extended π-electron systems have been a subject of interest in recent years (18). Of particular interest are conjugated π-electron polymers doped with charge transfer complexes exhibiting semiconducting or metallic properties (18). We have investigated the polymer poly(3-methylthiophene), which can be electropolymerized onto a platinum electrode yielding a conductive film. These films, however, when exposed to ambient conditions lose their conductivity and electrolytic activity after a few weeks (19,20). This polymer can also be synthesized by transition metal induced polymerization of 3-methyl-2,5-dilithiothiophene and 3-methyl-2,5-dibromothiophene at 0°C in dry tetrahydrofuran solution (21). The use of anhydrous cupric chloride yields the best results. When the resulting polymer is doped with iodine and exposed to moisture, this polymer displays very good conductivity (up to 40 S/cm) and an extraordinary degree of stability. The bulk copper concentration is about 30% by weight, as measured by atomic absorption analysis. When prepared under the same conditions using other transition metals, the resultant polymers exhibit poor conductivities ($\sim 10^{-7}$ S/cm) (22).

Our EXAFS studies have involved investigation of the chemical and structural form of the copper ions in this insoluble polymer matrix. The polymer samples, provided by Professors Harry B. Mark and Hans Zimmer, were presumed to be cross-linked via copper coordination to sulfur atoms of the thiophene rings. This would provide a 4 coordinate Cu-S environment (22). Polymers containing copper were synthesized from either anhydrous Cu^{I} (compound I) or Cu^{II} (compound II), and then were examined with XANES and EXAFS.

XANES spectra of compounds 1 and 2 display the same features with differing intensities with the features of 2 being shifted to lower energy with respect to 1. The envelopes of the extracted, filtered EXAFS from a single Fourier transform peak exhibited maxima at 5.6 and 5.1 $\AA^{-1}$ for 1 and 2 respectively. This is consistent with the position of the envelope maximum for a Cu-N model compound, Cu^{I}(2,9-dimethyl-1,10-phenanthroline)$_2BF_4$, $Cu(dmp)_2$. The envelope maximum of a Cu-S model compound, Cu^{II}(N,N-diethyldithiocarbamate)$_2$ or $Cu(dtc)_2$, occurs at 7.2 $\AA^{-1}$. Thus, the backscatterer is from the same row of the periodic table as nitrogen and is most likely oxygen from water absorbed by the polymer and not sulfur from the thiophene.

Curve fitting of the filtered EXAFS to model parameters extracted from the Cu-N and Cu-S compounds was used to further define the coordination environment. These results are presented in Table 2. For compound 1 the attempt to fit to a Cu-S model resulted in a negative coordination number and an unreasonable value of ΔE_o, showing that Cu-S coordination should be rejected. Cu-N modeling (we had no good Cu-O model available) for compound 1 resulted in reasonable bond distances and coordination numbers. For compound 2, Cu-N modelling results in a low value of the coordination number, suggesting a high level of disorder about copper. Attempts to model with sulfur neighbors give entirely unreasonable Cu-S bond lengths, and so, were rejected. Thus both the envelope shapes and curve fitting indicate that in these materials from Mark and Zimmer there is no sulfur coordination.

Table 2 - Copper Poly(3-Methylthiophene) Results

Sample	Model	Bond	CN	BL	ΔE_o	
Compound 1	$Cu(dmp)_2$	Cu-N	3.7	1.97	-2.5 eV	
	$Cu(dtc)_2$	Cu-S	-4.9	2.15	48.0 eV	
Compound 2	$Cu(dmp)_2$	Cu-N	2.3	1.97	-5.9 eV	
	$Cu(dtc)_2$	Cu-S	4.2	1.98	26.0 eV	

This study provides insight concerning the role of the copper in the conduction process. In the non-conductive system, the copper contained within the p(3-methylthiophene) matrix complexes water. This complexation causes a distortion in the orientation of the thiophene array, thereby disrupting the π-electron conductivity present in the absence of water.

Our work complements the previous, elegant work of Tourillon. We have reviewed that work (17) in our article for Chemical Reviews. Tourillon found that copper from aqueous solution could enter the polymer and remain oxygen coordinated until reduced electrochemically when it subsequently became sulfur coordinated. Clearly, EXAFS has proven extremely useful for characterizing this complex polymer system.

4. EXAFS Spectroelectrochemical Flow-Cell

We have shown that electrolysis offers a practical alternative to chemical generation of chosen oxidation states. For EXAFS measurements potential control may be necessary to maintain the oxidation state of the metal being observed, due to the highly reducing environment generated by secondary electrons produced by the intense synchrotron radiation. Work by Chance et al has shown that the use of a flowing stream of analyte solution can greatly reduce the time the complex spends bathed in X-rays, thereby minimizing destruction of the sample (23). We have built and evaluated a cell which combines both electrochemical potential control and a flowing analyte stream (24). A packed carbon-bed bulk electrolysis cell generates the desired metal oxidation state. The system consists of a closed loop of electrolyte solution containing the analyte of interest. The solution passes through the carbon-bed and subsequently through the path of the X-ray beam. A series of experiments has shown that complete oxidation and reduction of a 10 mM solution of $K_3Fe(CN)_6$ can be achieved with only one electrolysis pass.

One advantage of this design is the ability to electrolyze solutions outside the X-ray beam, avoiding the problems of electrode positioning. Performing electrolysis outside the X-ray beam will permit the use of analyte solutions of higher concentrations, since the rate of electrolysis may be increased by a working electrode which possesses a very large surface area. We can also make the solution flow cell quite thin (~0.5 mm), which will provide higher total transmission and thus a better signal to noise ratio for downfield calibration of the energy. This design is also easily adaptable to various beamline configurations. For example, the X-ray beam at line X-9A at NSLS (the National Biostructure PRT) is very wide (ca. 5.0 cm). Since the electrodes are not in the X-ray cell, it is relatively easy to construct a special cell which will take advantage of the full width of the beam. We believe that it should add considerable versatility to our experimental setups.

Another advantage of this particular experimental setup includes the ability to saturate the analyte solution with a particular gas while performing the experiment. This is accomplished through the use of a gas purged polyethylene jacket, surrounding the gas-permeable Teflon tubing which is used to transport the solution. This allows investigation of the effect(s) of on electrochemical reaction mechanisms. In the previous electrochemical cells we have used, we did not have the ability to easily and efficiently saturate the analyte solution with a particular gas and maintain this condition over time.

5. Structure of Metals in Amalgams.

Anodic stripping voltammetry is an extremely useful and sensitive technique for determining various metal ions in aqueous solutions (25-29). This technique is based upon the fact that when certain metals (e.g., In^{+3}, Tl^{+}, Cd^{+2}, Zn^{+2}, Ga^{+3}, Sn^{+2}, Pb^{+2}, Bi^{+3}) are reduced at a mercury electrode, they amalgamate and diffuse into the mercury. The net effect of this process is to preconcentrate these metals within the electrode, which typically improves the detection limits for their subsequent oxidation by approximately three orders of magnitude over conventional electrochemical techniques (26). Once preconcentrated in the mercury, the analyte is then quantified by either linear potential scan or differential pulse voltammetry.

The characteristics of amalgams have been extensively analyzed with a variety of techniques (26-30). The solubilities of various metals in mercury have been determined and are given in Table 3, column 2. Most of these

Table 3 - Feasibility of EXAFS Studies with Various Amalgams

Metal	Amount in Amalgam[a] (mMoles/cm^3)	Edge	Energy[b] (keV)	Penetration Depth[c] (μm)	Cross-Section (μMoles/cm^2)	Feasibility
Hg		L1	14.8			
		L2	14.2			
		L3	12.3			
In	67.0	K	27.9	3.83	25.66	102.63
Tl	28.0	L3	12.6	0.92	2.62	10.48
Cd	6.0	K	27.7	3.74	2.25	8.98
Zn	3.9	K	9.6	1.03	0.40	1.61
Ga	2.6	K	10.3	1.30	0.34	1.37
Ba	0.32	K	37.4	10.13	0.33	1.31
Sn	0.68	K	29.2	4.36	0.30	1.19
Pb	0.98	L3	13.0	1.00	0.01	0.39
Bi	0.90	L3	13.4	1.08	0.01	0.39
Na	3.64	K	1.0	0.06	0.02	0.08
K	1.31	K	3.6	0.13	0.02	0.07
Au	0.09	L3	11.9	2.21	0.02	0.08
Ag	0.04	K	25.5	2.99	0.01	0.04
Mg	1.72	K	1.3	0.06	0.01	0.04

a This value was calculated from the density of mercury at room temperature (13.5 g/cm^3) and the solubility of the metal in mercury (% weight) from reference 26.

b Values obtained from reference 30.

c Penetration depth into pure mercury at the given edge energy such that the transmittance (I/Io) was 0.8.

metals will form complexes as solid alloys with mercury at low temperatures (26,27). For Na, K, and Mg metal-mercury amalgamation occurs in the liquid, as well a solid alloy phase (26 p. 158). Similarly, for In and Tl a metal-mercury amalgam is formed at room temperature over a variety of compositional ranges for the relative metal/mercury content in the amalgam (26 pp. 169-170, 31). For Cd, Ba, Au, and Ag, an amalgam is present at room temperature but is assumed to result from solid phase precipitates suspended within the amalgam (26). Finally, the metals Zn, Sn, Pb, Bi are assumed to be randomly distributed as free atoms in amalgams above 0°C (26). Based upon electrochemical measurements, it has been proposed that several $metal_1$-$metal_2$ complexes will form in amalgams (25,26,29). The solubility of intermetallic compounds in mercury is frequently low and the solid phase separates (26,27 p.63). Interestingly, in many cases, structures of these complexes are not known. In certain cases X-ray diffraction studies have been used to estimate the structural parameters in these amorphous matrices (30). To our knowledge, amalgams have not been investigated previously with EXAFS.

a. Theoretical Feasibility of EXAFS Experiments on Amalgams

Our ability to study amalgams via EXAFS spectroscopy is fundamentally limited by absorption of the solvent (mercury). As shown in Table 3, the penetration depth of X-ray photons into pure mercury at the specified energy, such that transmittance is equal to 0.8, is on the order of micrometers. To calculate the penetration depth at which the solvent is 99% absorptive simply multiply column 5 by a factor of 22.0 [ln(0.01)/ln(0.8)]. This penetration depth was chosen to provide a crude index of feasibility. From our previous studies we were able to reliably interpret the EXAFS spectra down to 1 mM $[Ru(NH_3)_6]^{+3}$ when transmittance of the sample cell and solvent (H_2O) was ~0.8, the cross-section was 0.25 μMoles/cm^2 (32). By multiplying the maximum concentration of the metal in the amalgam (column 2, mmoles/cm^3) by the penetration depth (column 5, μm), the cross-section of non-mercury metal (μmoles/cm^2) when I/Io = 0.8 can be calculated easily as given in Table 3, column 6. From these data a feasibility coefficient can be determined by dividing the column 5 value by 0.25, where a value of 1.0 is approximately equivalent to the 1 mM $[Ru(NH_3)_6]^{+3}$ case previously studied (32). Based on these calculations, useful EXAFS measurements with saturated amalgams of In, Tl, Cd, Zn, Sn, Ba, and Ga should be feasible and may be possible with Pb and Bi but seem less likely to yield worthwhile results with Na, K, Au, Ag, Mg (See Table 3).

b. Preliminary EXAFS Spectroelectrochemistry on Zn-Hg Amalgam

The feasibility of EXAFS spectroelectrochemistry has been evaluated with a preliminary experiment on zinc. The choice of zinc was based on two factors. First, we have had considerable experience with the anodic stripping of Zn from mercury films (33). Second, success with zinc would suggest that experiments are possible for the entire top group of 7 metals in Table 3, which is enough to warrant a comprehensive study.

The experiment was performed in a flow cell that is a modification of our previously reported design (17) with reticulated vitreous carbon (RVC) as the working electrode. A peristaltic pump delivered 0.1 M acetate buffer pH 5.4 (pre-electrolyzed at a mercury pool electrode to remove trace metals) for rinsing the cell, Hg^{2+} in buffer for electrodepositing a mercury film at -0.2 V vs Ag/AgCl, or Zn^{2+} in buffer for depositing Zn^{o} at -1.3 V vs Ag/AgCl in mercury. All solutions were deoxygenated with nitrogen immediately prior to use. A mercury film was first deposited in situ on the RVC by flowing Hg^{2+} solution through the cell, the cell was then rinsed, and then the amalgam was formed by flowing the Zn^{2+} solution through the cell. The cell was then flushed with buffer to remove all Zn^{2+}, disconnected from the potentiostat, and tape sealed for X-ray absorption measurements which followed immediately. Because the cell had to be disconnected from the potentiostat during the X-ray experiment, precautions were taken to avoid stripping of the zinc from the mercury film via oxidation to Zn^{2+} by dissolved oxygen. During collection of X-ray spectra, the sample chamber containing the sealed cell was purged with helium. X-ray absorption spectra were obtained on the electrodeposited amalgam for zinc (edge energy 9660.7 eV) and mercury (edge energy 12,286 eV). Spectra were also recorded of samples of metallic Zn and liquid Hg and aqueous solutions of Zn^{2+} and Hg^{2+}.

EXAFS data for the electrochemically deposited Zn-Hg amalgam was extracted from 15 independently calibrated fluorescence spectra. A Fourier transform was calculated for the extracted EXAFS signal, resulting in a pseudo-radial distribution function (PRDF). The PRDF obtained for the Zn-Hg amalgam was compared to both empirical and theoretical phase and amplitude functions extracted from model compounds. Model compounds consist of: a) 13.5 mM Zn^{2+} in 0.1 M, pH 5.4 acetate buffer solution, b) zinc foil, c) 10.0 mM Hg^{2+} in 0.1 M, pH 5.4 acetate buffer solution and d) liquid mercury.

Zinc Analysis. Figure 4 is a superposition of normalized X-ray data for Zn^{2+} (highest peak), Zn-Hg amalgam (intermediate peak) and Zn^{o} (lowest peak).

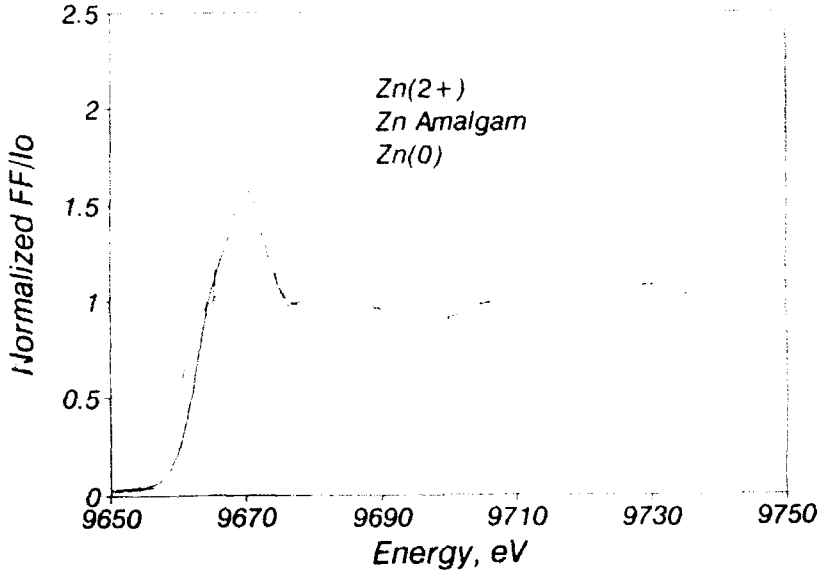

Figure 4

The inflection points of the edge rise for Hg-Zn amalgam occurs at 9662.8 eV, while those of Zn° and Zn^{2+} were found to occur at 9660.1 and 9665.6 eV respectively. The first maximum of both the Zn° and Zn^{2+} X-ray spectra is located at 9667 eV. For the Hg-Zn amalgam the position of the first maximum occurs at essentially the same energy. A feature observed in the Hg-Zn amalgam XANES region, which is different than that for Zn° and Zn^{2+}, is a prominent maximum in the normalized fluorescence signal at 9681.5 eV.

Following normalization of the X-ray fluorescence data, the EXAFS signal versus the photoelectron wave vector (**k** in $Å^{-1}$) was Fourier transformed to Å space, Fig. 5. The Fourier transform of the EXAFS signal for Zn-Hg amalgam indicated 2 regions of electron density surrounding the absorbing Zn atoms. The Fourier transform maxima are presented in Table 4.

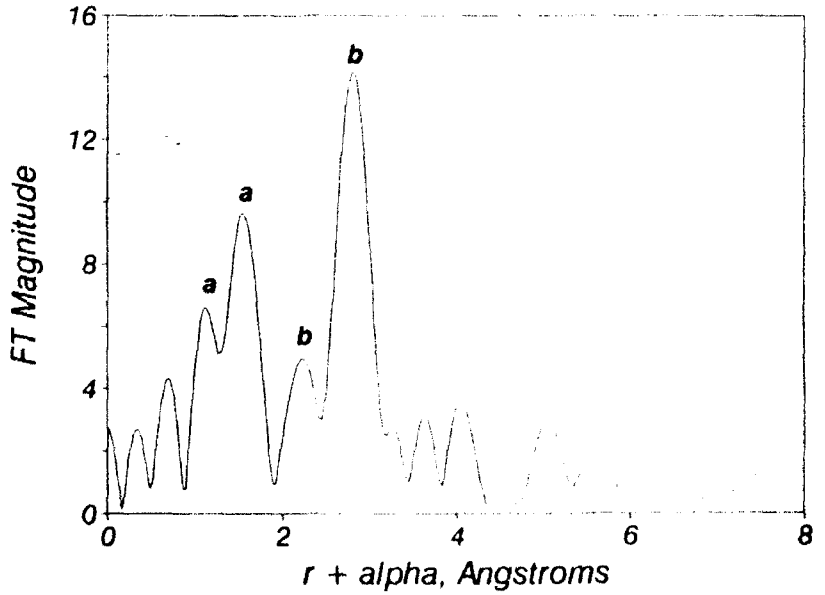

Figure 5

Table 4

Positions of Fourier Transform Maxima

for Zn-hg Amalgam at Zn Absorption Edge

$r + \alpha$ (in Å)	Height	
0.70	4.30	
1.13	6.59	a
1.55	9.65	a
2.23	4.95	b
2.81	14.13	b
3.26	2.76	
3.63	3.12	
4.04	3.57	

Two regions of the Fourier transform encompassing peaks **a** and **b** were isolated with Gaussian windows (width = 0.1 Å) and reverse transformed to **k**-space for comparison with model phase and amplitude functions. The first transform region was from 0.85 to 1.9 Å and included peaks **a**. The second region included only the peaks at 2.23 and 2.81 Å.

Spectra collected for zinc foil and $[Zn^{II}(H_2O)_6]^{2+}$ were normalized and Fourier transformed in the same manner as described above. Major maxima of the model Fourier transforms were located at 2.20 Å for Zinc foil and 1.59 Å for $[Zn^{II}(H_2O)_6]^{2+}$. Single regions of the PRDF incorporating the maxima above were Fourier filtered.

Comparisons of the 2 major backscattering regions of the Zn-Hg amalgam PRDF (labeled **a** and **b** in Table 4) were made with the data collected on the model compound. Region **a** is attributed to Zn-O interaction, based on its position in Å space and the shape of the filtered EXAFS envelope, both of which are essentially identical with that for the model. Region **b** is at a distinctively further distance than that of Zn-O and Zn-Zn. The filtered EXAFS envelope suggests backscattering contributions by an atom type of higher electron density than O or Zn, and is more similar to that expected for Hg. Attempts have been made to fit the filtered EXAFS spectra with theoretical phase and amplitude functions, resulting in distances that are considerably longer that that of a covalent Zn-Hg bond, 2.75 Å. The value of bond distance returned by our optimization of theoretical parameters is 3.0 Å.

The structure of elemental mercury is that of an eight coordinate Hg with bond distance of 3.0 Å according to X-ray diffraction experiments. This value is in line with the Zn-Hg distance which we found above. Thus it appears that the zinc atoms are substituting into the mercury structure with little disruption. The cavity into which the Zn fits is too large for contact as short as the covalent radii would suggest, 2.75 Å, and thus the zinc atoms rattle around in the hole. However the size mismatch seems to be not so great as to disrupt the Hg structure. The loading in the preliminary experiment was rather low. It will be interesting to determine whether the mercury structure is changed by increasing levels of Zn substitution prior to saturation.

Mercury Analysis. Fourier transform analysis of X-ray fluorescence data collected at the mercury L_{III} edge were uninterpretable. This was due to the high levels of noise relative to the mercury edge rise. Several factors combine to cause the significant decrease in the signal to noise ratio: a) the decrease in X-ray flux is approximately a factor of 2 as compared to the flux at the zinc edge energy, b) 4 complete **k**-scans were collected at the Hg L_{III} edge as compared to 15, collected at the Zn K edge and c) the μ_{norm} of Hg at its Hg L_{III} absorption edge, 12,280 eV, is 1.44, where μ_{norm} is equivalent to $(\mu_{above}-\mu_{below})/\mu_{below}$. The μ_{norm} of Zn at its K absorption edge is 6.27.

6. Non-Ideal Behavior of Spectroelectrochemical Nernstian Plots

Analysis of Nernstian plots has been shown to be a powerful technique for determining the formal redox potentials and electron stoichiometries of various electroactive species. However, in certain situations nonlinear Nernstian plots have been observed. Consequently, analysis by conventional methodologies results in erroneous estimation of these redox parameters. For single site redox species, the most likely explanation of the observed deviation involves the spectral overlap of two or more chemically independent redox couples. We have explored the chemical basis for the observed deviation and presented a model which predicts this behavior. The validity of the chemically independent redox model was demonstrated using thin-layer spectroelectrochemistry with two well characterized spectroelectrochemical systems: ferricyanide and σ-tolidine (34).

7. Conclusions

In sum, during the three years of AFOSR support, we have been able to demonstrate the applicability of EXAFS spectroelectrochemistry to the study of coordination compounds that are immobilized in thin films of ionically conducting polymers on electrode surfaces, metal ions in electrically conducting polymers, and electroactive films on electrode surfaces. Unique cell designs have been developed to deal with the inherently poor sensitivity of the EXAFS experiment, while retaining adequate electrochemical control to enable facile conversion and maintenance of oxidation state. To develop and demonstrate this methodology, we have used electrochemical and polymer systems currently of general interest to the electrochemical community: Nafion, p(DMDAAC), Prussian Blue, and p(3-methylthiophene). In each case, EXAFS has provided structural information that was previously unknown and which could be useful in the further understanding and development of those chemical systems.

8. Publications and Presentations.

We have published the following papers under the support of the Air Force:

1) In Situ Observation of Copper Redox in a Polymer Modified Electrode Using EXAFS Spectroelectrochemistry. R.C. Elder, C.E. Lunte, A.F.M.M. Rahman, J.R. Kirchhoff, H.D. Dewald, W.R. Heineman, J. Electroanal. Chem. **240**, 361-364 (1988).

2) The Electrochemistry of Hemin in DMSO. R.S. Tieman, L.A. Coury, Jr. Kirchhoff, W.R. Heineman, J. Electroanal. Chem. **281**, 133-145 (1990).

3) EXAFS Spectroelectrochemistry. L.R. Sharpe, R.C. Elder, W.R. Heineman, Chem. Rev. **90**, 705-722 (1990).

4) EXAFS Solid-State Spectroelectrochemistry: The Effects of Supporting Electrolyte on the Structure of $Cu(bcp\text{-}s)_2$. D.H. Igo, R.C. Elder, W.R. Heineman. J. Electroanal. Chem., in press. (Appendix I).

5) Non-Ideal Behavior of Nernstian Plots from Spectroelectrochemistry Experiments. E.W. Kristensen, R.C. Elder, W.R. Heineman. J. Electroanal. Chem., in press. (Appendix III).

6) Development of a Bulls-Electrolysis Flow-Cell System for Use in UV-Visible and X-Ray Absorption Spectroelectrochemical Analysis. D.H. Igo, R.C. Elder and W.R. Heineman, Anal. Chem., submitted. (Appendix II).

The following talks have been presented on our EXAFS spectroelectrochemistry under Air Force support:

1) EXAFS Spectroelectrochemistry of Cu(DMP) Complexes Incorporated Into Nafion on a Carbon Electrode. C.E. Lunte*, K.F. Siddiqui, J.R. Kirchhoff, R.C. Elder, and W.R. Heineman. Symposium on Electrochemistry--Chemically Modified Electrodes II, Pittsburgh Conference, New Orleans, LA, February 22-26, 1988.

2) EXAFS Spectroelectrochemistry as an In-Situ Probe of Polymer Coated Electrodes. L.R. Sharpe, D.H. Igo, C.E. Lunte, A.F.M.M. Rahman, J.R. Kirchhoff, H.D. Dewald, W.R. Heineman, and R.C. Elder*. Symposium on Photochemical and Electrochemical Surface Science: Microstructural Probes of Electrode Processes-I, 197th National ACS Meeting, Dallas, TX, April 9-14, 1989.

3) EXAFS Spectroelectrochemistry. W.R. Heineman*, R.C. Elder, L.R. Sharpe, D.H. Igo, D.M. Caster, C.E. Lunte, and H.D. Dewald. US/Japan Seminar on Spectroscopic Characterization of Electrode Processes, Honolulu, HI, June 6-9, 1989.

4) EXAFS Structural Studies on Technetium and Rhenium Diphosphonates. J.L. Martin, J. Yuan, K. Libson, R.C. Elder, W.R. Heineman, and E. Deutsch*. The Society of Nuclear Medicine 36th Annual Meeting, St. Louis, MO, June 13-16, 1989.

5) EXAFS Spectroelectrochemistry. W.R. Heineman*, R.C. Elder, L.R. Sharpe, D.H. Igo, D.M. Caster, C.E. Lunte, and H.D. Dewald. ISE Pre-Symposium, Sendai, Japan, September 15-16, 1989.

6) EXAFS Spectroelectrochemistry of Metal Complexes in Polymer Films on Electrode Surfaces. D.H. Igo, L.R. Sharpe, R.C. Elder, W.R. Heineman*. 200th National ACS Meeting, Washington, D.C., August 26-31, 1990.

7) EXAFS Spectroelectrochemistry of Copper(Bathocuproine Disulfonic Acid)$_2$ *in a Semi-rigid Poly(DMDAAC) Matrix.* D.H. Igo*, R.C. Elder, W.R. Heineman. Modern Techniques in Electroanalysis I, 17th annual FACSS Meeting, Cleveland, OH, October 7-12, 1990.

Literature

1) Whiteley, L.D.; Martin, C.R.: Perfluorosulfonate Ionomer Film Coated Electrodes as Electrochemical Sensors: Fundamental Investigations. Anal. Chem. 59, 1746-1751 (1987).

2) Kristensen, E.W.; Kuhr, W.G.; Wightman, R.M.; Temporal Characterization of Perfluorinated Ion Exchange Coated Microvoltammetric Electrodes for in Vivo Use. Anal. Chem. 59, 1752-1757 (1987).

3) Elder, R.C.; Lunte, C.E.; Rahman, A.F.M.M.; Kirchhoff, J.R.; Dewald, H.D.; Heineman, W.R.: In Situ Observation of Copper Redox in a Polymer Modified Electrode Using EXAFS Spectroelectrochemistry. Electroanal. Chem. 240, 361-361 (1988).

4) Jernigan, J.C.; Chidsey, C.E.D.; Murray, R.W.: Electrochemistry of Polymer Films Not Immersed in Solution: Electron Transfer on an Ion Budget. J. Am. Chem. Soc. 107, 2824-2826 (1985).

5) Oliver, B.N.; Egekeze, J.O.; Murray, R.W.: "Solid-State" Voltammetry of a Protein in a Polymer Solvent. J. Am. Chem. Soc. 110, 2321-2322 (1988).

6) Tieman, R.S.; Heineman, W.R.: Fabrication and Characterization of a Platinum/Ceramic Electrochemical Sensor. Sensors and Actuators, B, 5, 121-127 (1991).

7) Geng, L.; Reed, A.; Kim, M.H.; Woster, T.T.; Oliver, B.N.; Egekeze, J.; Kennedy, R.T.; Jorgenson, J.W.; Parcher, J.F.; Murray, R.W.: Chemical Phenomena in Solid-State Voltammetry in Polymer Solvents. J. Am. Chem. Soc. 111, 1614-1619 (1989).

8) Tieman, R.S.; Heineman, W.R.; Johnson, J.; Sequin, R.: Oxygen Sensors Based on the Ionically Conductive Polymer Poly(Dimethyldiallylammonium Chloride). Sensors and Actuators, B, 8, 199-204 (1992).

9) DeCastro, E.S.; Huber, E.W.; Villarroel, D.; Galiatsatos, C.; Mark, J.E.; Murray, P.T.; Heineman, W.R.: Electrodes with Polymer Network Films Formed by γ-Irradiation Cross-Linking. Anal. Chem. 59, 134-139 (1984).

10) Huber, E.W.; Heineman, W.R.: Role of Monomer in γ-Irradiated Dimethyldiallylammonium Chloride Modified Electrodes. Anal. Chem. 60, 2467-2472 (1988).

11) Igo, D.H.; Elder, R.C.; Heineman, W.R.: Solid-State EXAFS Spectroelectrochemistry: The Effects of Supporting Electrolyte on the Structure of $Cu(bcp\text{-}2)_2^{3-}$. J. Electroanal. Chem., 281, 45-57 (1991).

12) Lange's Handbook of Chemistry (Dean, J.A., ed.) (1979) 12, Chapter 10, 84.

13) Ellis, D.; Eckhoff, M.; Neff, V.D.: Electrochromism in the Mixed-Valence Hexacyanides. 1. Voltammetric and Spectral Studies of the Oxidation and Reduction of Thin Films of Prussian Blue. J. Phys. Chem. 85, 1225-1231 (1981).

14) Buser, H.J.; Schwarzenbach, B.; Petter, W.; Ludi, A.: The Crystal Structure of Prussian Blue: $Fe_4[Fe(CN)_6]_3 \cdot xH_2O$. Inorg. Chem. **16**, 2704-2710, (1977).

15) Teo, B.-K.: Novel Method for Angle Determination by EXAFS via a New Multiple-Scattering Formalism. A. Am. Chem. Soc. **103**, 3990-4001 (1981).

16) Lundgren, C.A.; Murray, R.W.: Observations on the Composition of Prussian Blue Films and Their Electrochemistry. Inorg. Chem. 27, 933-939, (1988).

17) Sharpe, L.R.; Elder, R.C.; Heineman, W.R.: EXAFS Spectroelectrochemistry. Chem. Rev. **90**, 705-722 (1990).

18) Waltman, R.J.; Bargon, J.; Diaz, A.F.: Electrically Conducting Polymers: A Review of the Electropolymerization Reaction, of the Effects of Chemical Structure on Polymer Film Properties, and of Applications Towards Technology. Can. J. Chem. **64**, 76-95 (1986).

19) Waltman, R.J.; Bargon, J.; Diaz, A.F.: Electrochemical Studies of Some Conducting Poly-Thiophene Films. J. Phys. Chem. **87**, 1459-1463 (1983).

20) Tourillon, G.; Barnier, F.: Stability of Conducting Polythiophene and Derivatives. J. Electrochem. Soc. **130**, 2042-2043 (1983).

21) Amer, A.; Zimmer, H.; Mulligan, K.; Mark, Jr., H.: Polymerization of 3-methyl-2,5-dibromothiophene Utilizing n-Butyl Lithium and Copper(II) Chloride. Journal of Polymer Science: Polymer Letters Edition **22**, 77-82 (1984).

22) Czerwinski, A.; Cunningham, D.; Amer, A.; Schrader, J.; Van Pham, C.; Zimmer, H.; Mark, Jr., H.; Pons, S.: The Electrochemical-Behavior in Aqueous Media of Conducting Polymers. J. Electrochem. Soc. **134**, 1158-1164 (1987).

23) Ayene, S.I.; Naqui, A.; Chance, B.: Sample Damage at BNL/NSLS on Beamline X-9A, National Synchrotron Light Source Annual Report 1987 p. 3.49.

24) Igo, D.H.; Elder, R.C.; Heineman, W.R.: Development of a Bulk-Electrolysis Flow Cell System for Use in UV-Visible and X-Ray Absorption Spectroelectrochemical Analysis. Anal. Chem. **63**, 2535-2539 (1991).

25) E. Barendrecht, in Electroanalytical Chemistry, Vol. 2 (A.J. Bard, ed.), Marcel Dekker, New York, 1967, pp. 53-109.

26) M. Kozolvsky and A. Zebreva, Intermetallic Compounds in Amalgams, in Progress in Polarography, Vol. 3, (P. Zuman and L. Meites, ed.), Wiley-Interscience, New York, 1972, pp. 157-194.

27) A.F. Trotman-Dickenson (ed.), Comprehensive Inorganic Chemistry, Vol. 3, Pergamon Press, London, 1973, p. 283-285.

28) F. Vydra, K. Stulik and E. Julakova, Electrochemical Stripping Analysis, Halsted Press, New York, 1976.

29) W. Heineman, H. Mark, and J. Wise, Electrochemical Preconcentration in Laboratory Techniques in Electroanalytical Chemistry, (P. Kissinger and W. Heineman, eds.) Marcel Dekker, New York, 1984, pp. 499-538.

30) Smallmann, R.E.; Frost, B.R.T.: An X-Ray Investigation of the Structure of Liquid Mercury and Liquid Mercury-Thallium Alloys. Acta Met. 4, 611-618 (1956).

31) Veigel, W.J., Photon Cross Sections from 0.1 Kev to 1 MeV for Elements Z=1 to Z=94, Atomic Data Tables, 5, 51-111 (1973).

32) Dewald, H.D.; Watkins, J.W.; Elder, R.C.; Heineman, W.R.: Development of Extended X-Ray Absorption Fine Structure Spectroelectrochemistry and Its Application to Structural Studies of Transition-Metals in Aqueous Solution. Anal. Chem. 58, 2968-2975 (1986).

33) Roston, D.A.; Brooks, E.E.; Heineman, W.R.: Elimination of Intermetallic Compound Interferences in Twin-Electrode Anodic Stripping Voltammetry. Anal. Chem. 51, 1728 (1979).

34) Non-Ideal Behavior of Nernstian Plots from Spectroelectrochemistry Experiments. E.W. Kristensen, R.C. Elder, W.R. Heineman, J. Electroanal. Chem., in press, (Appendix III).